

Towards Less Constrained Macro-Neural Architecture Search

Vasco Lopes

NOVA Lincs, Universidade da Beira Interior

vasco.lopes@ubi.pt

Luís A. Alexandre

NOVA Lincs, Universidade da Beira Interior

luis.alexandre@ubi.pt

Abstract

Networks found with Neural Architecture Search (NAS) achieve state-of-the-art performance in a variety of tasks, out-performing human-designed networks. However, most NAS methods heavily rely on human-defined assumptions that constrain the search: architecture's outer-skeletons, number of layers, parameter heuristics and search spaces. Additionally, common search spaces consist of repeatable modules (cells) instead of fully exploring the architecture's search space by designing entire architectures (macro-search). Imposing such constraints requires deep human expertise and restricts the search to pre-defined settings. In this paper, we propose LCMNAS, a method that pushes NAS to less constrained search spaces by performing macro-search without relying on pre-defined heuristics or bounded search spaces. LCMNAS introduces three components for the NAS pipeline: i) a method that leverages information about well-known architectures to autonomously generate complex search spaces based on Weighted Directed Graphs with hidden properties, ii) a evolutionary search strategy that generates complete architectures from scratch, and iii) a mixed-performance estimation approach that combines information about architectures at initialization stage and lower fidelity estimates to infer their trainability and capacity to model complex functions. We present experiments showing that LCMNAS generates state-of-the-art architectures from scratch with minimal GPU computation. We study the importance of different NAS components on a macro-search setting. Code for reproducibility is public at <https://github.com/VascoLopes/LCMNAS>.

1. Introduction

Advances in deep learning algorithms obtained remarkable progress in various problems, mainly due to the ingenuity and engineering efforts of human experts that exhaustively designed and engineered powerful architectures. Convolutional Neural Networks (CNNs) have been extensively applied with great success to different image problems, obtaining unprecedented results [24,28,53]. However,

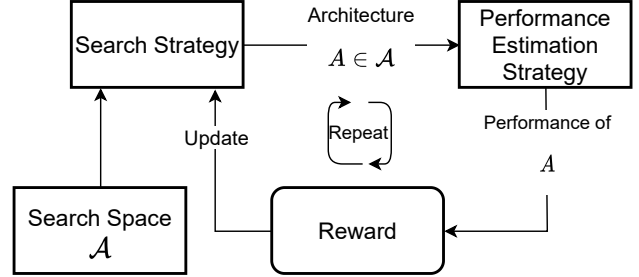


Figure 1. Generalist NAS flow. A controller generates an architecture A from the space of possible architectures, \mathcal{A} , which is then evaluated, and its performance is used as reward to update the controller. In this paper, we propose methods for all components: search space, search strategy, performance estimation strategy.

designing CNNs is a gruelling endeavour that heavily relies on human expertise. Thus, automating this process became logical [21]. Neural Architecture Search (NAS) intends to automate architecture engineering and design [13]. NAS methods have successfully been applied to image classification tasks [5,36,38,40,71], semantic segmentation [32,33], object detection [8] and image generation [14,15], consistently achieving state-of-the-art results. Generally, NAS methods are composed of three components: i) the search space, which defines the pool of possible operations and ultimately, the type of networks that can be designed; ii) the search strategy, which is the approach used to explore the search space and generate architectures; and iii) the performance estimation strategy, which is how the generated architectures are evaluated during the search process. A general interaction between the different NAS components is presented in Fig. 1. Architecture search can either be performed using micro or macro-search. In micro-search, methods focus on creating cells or blocks that are replicated multiple times, whereas, in macro-search, NAS methods try to evolve entire network architectures. An increasing number of NAS methods have been proposed, where the focus has been targeted at optimizing the search to reduce the required computations, and at the same time, increase the performance of the generated architectures [13,37,50].

NAS methods perform well on designing CNNs, but they still encounter several drawbacks: i) search spaces are heavily dependent on human-definitions, which are usually small and contain forced operations; ii) the search is mostly cell-based, where NAS methods search for small cells that are later replicated in a human-defined outer-skeleton; iii) architecture-related parameters, such as the number of layers, inner-layer parameters (e.g., the kernel size, output channels), the final architecture skeleton, fixed operations, and head and tail of the final architectures are usually defined by the authors; and iv) the time required to perform macro-search (search entire networks) is still considerable. By forcing rules and carefully designing search spaces, there is undoubtedly human biases introduced in the loop, which was found to often impact more the final result of the architectures than the search strategy itself, as it pushes NAS to constrained search spaces with very narrow accuracy ranges [60, 67], thus jeopardizing the generalization of the NAS methods, even to more simpler settings [11, 29]. Moreover, the idea of heading to NAS to avoid needing deep knowledge regarding architecture design ends up being frustrated since a similar degree of human involvement is required as when designing isolated CNN architectures.

In this work, we propose **LCMNAS** - Towards **Less Constrained Macro-Neural Architecture Search**, a NAS method that: i) autonomously generates complex search spaces by creating Weighted Directed Graphs with hidden properties (WDG) from existing architectures to leverage information that is the result of years of expertise, practice and trial-and-error; ii) performs macro-architecture search, without explicitly defined architecture’s outer-skeletons, restrictions or heuristics; and iii) uses a mixed-performance strategy for estimating the performance of the generated architectures, that combines information about the architectures at initialization stage with information about their validation accuracy after a partial train on a partial data set. Our extensive experiments show the importance of different NAS components in a macro-search setting and discuss their usability.

The main contributions of this paper are summarized as follows:

- We propose a search space design method that leverages information about existing CNNs to autonomously design complex search spaces.
- An evolutionary search strategy that performs macro-search to design entire architectures from scratch, without forcing an architecture shape or structure, or well-engineered protocols. More, the proposed search strategy goes beyond solely designing architectures to also determining the hyper-parameters associated with each layer.
- A mixed-performance estimation mechanism that cor-

relates untrained architecture scores with their final performance, and combines it with partial train to infer the architecture’s trainability with minimal training. This allows for remarkable computation efficiency improvements.

- Experiments demonstrate that the architectures found with LCMNAS achieve state-of-the-art results by directly searching on CIFAR-10, CIFAR-100 and ImageNet16-120 data sets.
- Extensive ablation studies showing the applicability of different NAS components, e.g., zero-cost proxy estimation, in a macro-search setting and evaluation of standard practices, such as transferring searched architectures to new data sets, and architecture diversity via ensembling.
- Finally, we extract insights about architecture design based on the decisions made by LCMNAS that might inspire future research.

2. Related Work

Neural Architecture Search was initially formulated as a Reinforcement Learning (RL) problem, where a controller was trained to sample more efficient architectures over time [74]. Albeit excellent results, it required more than 60 years of GPU computation to search for an architecture. Follow-up work [75], proposed a cell-based search in a search space of 13 operations. To form entire architectures, generated cells were stacked according to pre-defined rules. Even though it still required more than 2000 days of GPU computation, it prompted many proposals to focus on cell-based designs. Cell-based search spaces are generally represented as Directed Acyclic Graphs (DAGs), where nodes represent tensors and edges are operations [13]. Different NAS strategies have been proposed to improve upon initial results, including novel RL strategies [2, 17, 47, 73] and evolutionary algorithms, where architectures are designed using evolution via cross-over and mutations [35, 37, 41, 48, 65].

Recently, differentiable-based NAS attracted interest by designing cell-based architectures through relaxing a discrete search space optimizing the search process using efficient gradient descent [5, 7, 36, 64, 66, 71]. DARTS initially proposed the use of a bi-level gradient optimization to search for architectures and weights directly [36]. DARTS search space is popular, being used in the surrogate benchmark NAS-Bench-301 [54]. Common search spaces include tabular benchmarks, such as NAS-Bench-101 with 3 operations [68] and NAS-Bench-201 benchmark with 5 operations [11], and the NASNet [48] with 8 operations. These search spaces are focused on the design of cell-based architectures.

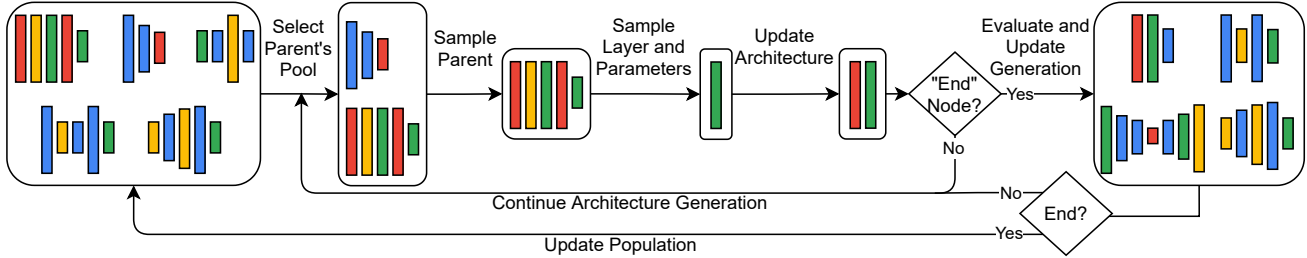


Figure 2. Illustration of one iteration of LCMNAS. Architectures are represented with varying width and bar’s length to illustrate their diversity. The process shows the sequential design of sampling one layer and associated hyper-parameters for an architecture. Designing and evaluating architectures happens several times in a generation. The whole search ends when the evolution reaches a final generation.

Methods that perform macro-search are closely related to our work. NAS [74], ENAS [47], MetaQNN [2] and Net Transformations [4] performed macro-search using RL strategies. Evolutionary algorithms have also been proposed [12, 43, 49], where architectures are designed through the use of mutations. More, Network Morphism has also been studied for macro-search, where morphisms are applied to initial architectures [12]. RandGrow does this based on random-search [18], and a follow-up work, Petridish, used gradient boost to further improve the method [19]. Differently, EPNAS performs macro-search by Sequential Model-Based Optimization (SMBO) with weight sharing. However, macro-search NAS methods tend to strictly force human-defined rules, such as well-designed search spaces with very narrow accuracy ranges, architecture’s outer-skeleton, their size (number of layers) and hyper-parameter heuristics. These forced rules have been shown to influence more the final accuracy of the architectures than the search itself [29, 60, 67]. NAS [74] and ENAS [47] also design additional filters for the best architectures by hand. From the proposed macro-search NAS methods, those that constrain the search less tend to be inefficient. LEMONADE required 80 GPU days of computation [12], and large-scale evolution required 2750 GPU days [49].

Performance Estimation Strategy Evaluating the performance of generated architectures is the most costly component of a NAS method. Albeit training an architecture for a large number of epochs is the most reliable mechanism to rank it, this is extremely inefficient [34, 74, 75]. Several performance estimation strategies have been proposed to improve the search procedure. Weight sharing reduces the evaluation time by sharing weights across generated architectures [5, 47, 64]. Low-fidelity estimates reduce the training time by training for fewer epochs or using subsets of the data, [72]. Model-based predictors predict the final validation accuracy of an architecture based on its encodings [23, 30, 61]. Zero-cost proxies look at architectures at initialization stage, and calculate statistics that correlate with the architecture’s final validation accuracy [6, 39, 45]. White et. al. provide a comprehensive evaluation of 31

different performance estimation strategies [62], showing that optimal results are obtained when combining multiple strategies.

To push NAS to less constrained settings, we focused on designing methods for macro-search. We propose a representation of complex search spaces as WDG, an evolutionary strategy that designs architectures from scratch, and an efficient mixed estimation-performance method that combines the evaluation of an architecture trainability through low fidelity estimates and its capability to model complex functions at initialization stage using a zero-proxy estimator.

3. Proposed Method

3.1. Search Space

Search spaces are commonly defined as DAGs, where edges represent operations and nodes are tensors. The goal is to design cells that are repeated to form entire architectures, where the operations pool and architectures outer-skeletons are pre-defined by the users. However, this has been shown to force the search to very narrow accuracy ranges and to compromise the generalization beyond the evaluated data sets [29, 60, 67], and at the same time, requires deep expertise to apply to new problems.

Instead of explicitly defining a search space, we propose a novel method to automatically design search spaces without requiring human-specified settings by leveraging information about existing CNNs, which are the result of years of expertise, practice and many trial-and-error experiments. For this, we extend the use of DAGs, and represent existing CNNs as Weighted Directed Graphs with hidden properties: $G(Q, E, H)$, where Q is the set of nodes, E the set of edges and associated weights as state-transition probabilities, and H is the set of inner states of the nodes and associated probabilities.

To generate a WDG, $G(Q, E, H)_i$, one can define a mapping from the input x to an output y using an architecture, n_i , as $w_{n_i}(x)$. This mapping is the result of feed-forwarding the input x through a set of layers. By looking

at the mapping, a summary of n_i can be generated and used to produce the sets \mathbf{Q} and \mathbf{E} . To obtain the state-transition probability between two layers, $P(l_i|l_j)$, we divide the frequency of the state-transition $C(l_i, l_j)$ by the sum of frequencies of state-transitions from l_i to any other possible layer: $C(l_i, l_k), k = 1, \dots, K$, where K is the number of layers that appear after the layer l_i in the summary. Thus, the weight of an edge $e(l_i, l_j) \in \mathbf{E}$ is given by:

$$e(l_i, l_j) = P(l_i|l_j) = \frac{C(l_i, l_j)}{\sum_{k=1}^K C(l_i, l_k)} \quad (1)$$

The inner-states $h_i \in \mathbf{H}$ of a layer l_i , represent all possible parameters and associated values that appear in the CNN, e.g., for a convolutional layer, possible inner-states will be the output channels and kernel sizes and their associated probabilities. The inner-states of a layer $h \in \mathbf{H}$ are calculated similarly to the edges between nodes. For each possible component (e.g., kernel size), the probability associated with the value (e.g., kernel size 3×3), is calculated based on the frequency of that value divided by all possible values for that specific parameter. Note that a start and end node are added to all WDG to allow the search strategy to stop the search.

In the end, the search space, \mathcal{A} , is represented by all CNNs in the form of their WDGs and fitness for the given problem (see Section 3.3), $(\mathbf{G}(\mathbf{Q}, \mathbf{E}, \mathbf{H}), f)$, such that $\mathcal{A} = \{(\mathbf{G}(\mathbf{Q}_1, \mathbf{E}_1, \mathbf{H}_1), f_1), \dots, (\mathbf{G}(\mathbf{Q}_N, \mathbf{E}_N, \mathbf{H}_N), f_N)\}$, where N is the number of CNNs used to create the initial search space.

By using WDGs to represent CNNs, the proposed method extracts information about the combination of layers and their associated parameters. This allows NAS methods to extract past information and move beyond solely designing layers and using heuristics to select their parameters, to a broader search, where the focus is on designing entire architectures by finding both the layers and associated parameters. The method is, thus, inferring human-expertise directly from the search space without requiring human intervention in the form of defined settings or parameters. Moreover, by combining an evaluation of CNNs for the problem in the form of the fitness f , to the the WDGs, $\mathbf{G}(\mathbf{Q}, \mathbf{E}, \mathbf{H})$, the search strategy can guide the search more efficiently.

3.2. Search Strategy

We propose an evolutionary strategy that leverages information present in the WDGs, to generate architectures from scratch, without requiring heuristics or pre-defined schemes for the layer's hyper-parameter and architecture structures. Architectures are generated by sequentially sampling layers and associated hyper-parameters from the individuals present in \mathcal{A} . To generate a layer, l_i , a pool of parents, $D \subseteq \mathcal{A}$, is sampled based on the presence of the

last sampled layer l_{i-1} on all individuals from \mathcal{A} (l_1 is the start node). An individual $j \in D$, is selected to be the parent of the layer l_i by performing a ranked roulette wheel selection using the fitness of the individuals in D . This ensures that individuals in D that have high fitness scores do not dominate the selection, thus promoting exploration of the search space. After an individual $j \in D$ is selected as parent, a layer l_i is sampled using Fitness Proportionate Selection (FPS) using as weights the state-transition probabilities present in $\mathbf{G}(\mathbf{Q}_j, \mathbf{E}_j, \mathbf{H}_j)$, denoted as $P(l_t|l_{i-1})$, $t = 1, \dots, T$, where T is the number of the nodes that have an input state-transition from l_{i-1} . Finally, the components of the layer sampled, e.g., output channels, are also sampled using FPS from the inner-state of the layer sampled l_i from the sampled parent $j \in D$. The iterative process of sampling layers from different parents promotes diversity for the generated architecture. Furthermore, following the insights obtained by evolutionary NAS methods like large-scale evolution [48], regarding the benefits of applying mutations, LCMNAS also employs a mutation process: when a convolutional layer is sampled, it has a fixed probability, 50%, of being mutated to a skip-connection.

The evolutionary strategy is performed for g generations, where at each generation, p individuals are generated and the top 15% architectures from the parents population are passed to the next generation through elitism. Fig. 7 illustrates the evolutionary process, where architectures are represented with varying width and bar lengths, and colors serve the purpose of differentiating between layers but do not represent specific types.

3.3. Performance Estimation Mechanism

The greatest NAS bottleneck is the evaluation of the generated architectures, as fully training each one is extremely expensive, requiring thousands of GPU days of computation [74, 75]. Accordingly, we propose a mixed-performance estimation approach that combines low fidelity estimates with zero-cost proxies to speed up the evaluation, while at the same time ensuring that the resulting score is a reliable approximation of the fully trained architecture ranking.

First, the proposed method evaluates the trainability of a generated architecture in a partial data set for a small number of epochs, e . Let us denote the objective function that calculates the accuracy of the architecture n_i on a small validation set, d^{valid} by $\mathcal{O}(n_i, d^{valid})$. The validation accuracy is used as an indication if the architecture is capable of learning from the small number of examples shown, which ultimately can be used to distinguish between architectures that can be trained efficiently from those that can't. The proposed method then looks at the capability of the untrained architecture at initialization stage to model complex functions, through Jacobian analysis [39, 45]. For this, one can define a mapping from the input $\mathbf{x}_i \in \mathbb{R}^D$, through the net-

work, $w(\mathbf{x}_i)$, where \mathbf{x}_i represents an image that belongs to a batch \mathbf{X} , and D is the input dimension. Then, this mapping can be computed by: $\mathbf{J}_i = \frac{\partial w(\mathbf{x}_i)}{\partial \mathbf{x}_i}$.

To evaluate how an architecture behaves for different data points, we calculate the Jacobian \mathbf{J} for different data points, \mathbf{x}_i , of the batch \mathbf{X} , $i \in 1, \dots, I$:

$$\mathbf{J} = \begin{pmatrix} \frac{\partial w(\mathbf{x}_1)}{\partial \mathbf{x}_1} & \frac{\partial w(\mathbf{x}_2)}{\partial \mathbf{x}_2} & \dots & \frac{\partial w(\mathbf{x}_I)}{\partial \mathbf{x}_I} \end{pmatrix}^\top \quad (2)$$

Then, the correlation matrix, Σ_J , allows the analysis of how the architecture models the target function at different data points, where ideally, for different images, the architecture would have different \mathbf{J} values, thus resulting in low correlated mappings. Then, we can use KL divergence to score an architecture based on the eigenvalues of its correlation matrix. Let $\sigma_{J,1} \leq \dots \leq \sigma_{J,V}$ be the V eigenvalues of Σ_J . The untrained architecture can be scored as:

$$s = 1 \times 10^4 / \sum_{i=1}^V [\log(\sigma_{J,i} + k) + (\sigma_{J,i} + k)^{-1}], \quad (3)$$

where $k = 1 \times 10^{-5}$.

The proposed mixed-performance estimation approach calculates the fitness, f , by combining the evaluation of the architecture's trainability, using $\mathcal{O}(n_i, d^{valid})$, and their capability of modeling complex functions, using s by:

$$f_{n_i} = (1 - \lambda) \times \mathcal{O}(n_i, d^{valid}) + \lambda \times s \quad (4)$$

where λ serves the purpose of giving different weights to each component. When $\lambda = 0$, the fitness of an architecture is only based on the trainability of the network by looking at the validation accuracy using a partial train on a partial data set, $\mathcal{O}(n_i, d^{valid})$. When $\lambda = 1$, the architecture's capability of modeling complex functions at initialization stage is the only considered factor. In the conducted experiments (see Section 4) we evaluate the importance of λ .

4. Experiments

4.1. Data Sets

We directly search and evaluate the proposed method on three data sets: CIFAR-10 [25], CIFAR-100 [25] and ImageNet16-120 [11]. CIFAR-10 and CIFAR-100 both contain 50K training images and 10k test images with 32×32 pixel sizes, having 10 and 100 classes, respectively. ImageNet16-120 is a down-sampled variant of ImageNet, where all images have 16×16 pixels and only considers the first 120 classes of ImageNet, resulting in 151.7K training images, 3K validation images and 3K test images. For searching purposes, we generated a partial data set for all the data sets. Here, 8% and 2% of the training set were randomly sampled to serve as partial training and partial validation sets. For training the final searched architectures, we use the original, entire splits.

4.2. Final Training

To evaluate the final architecture, we follow common training procedures [36, 47, 48]. However, we do not take advantage of drop path and other well-engineered training protocols that hide the contributions of the search strategy and the search space [67], or that require forcing architectures to have specific schemes, e.g., auxiliary towers [27], as suggested by NAS best practices in order to showcase the true contributions of the proposed method [29, 31, 60, 67].

Final architecture is trained for 600 epochs with batch size 96. We use SGD optimization, with an initial learning rate, $\eta = 0.025$ annealed down to zero following a cosine schedule without restart [42], momentum of 0.9 [56], weight decay of 3×10^{-4} and cutout [10].

4.3. Search Space

To create the search space, we used all the 34 models present in TorchVision version 0.8 [1], and generated their WDGs and associated fitness. Further details of the models can be found in the supplementary materials. The resulting search space is extremely large, composed of 19 possible operations: $\{1 \times 1, 3 \times 3, 5 \times 5, 7 \times 7, 11 \times 11\}$ convolution; $\{2 \times 2, 3 \times 3\}$ max pooling; 2×2 average pooling; $\{1 \times 1, 6 \times 6, 7 \times 7\}$ adaptive average pooling, $\{4096, 1024, 1000\}$ linear, $\{0.2, 0, 5\}$ dropout and skip-connection. In the WDGs, $\mathbf{G}(\mathbf{Q}, \mathbf{E}, \mathbf{H})$, the inner-state choices for a given node, e.g., the output channels for a convolutional layer, are also present.

As we do not bound the search either by defining architecture's outer-skeletons or the number of layers, the search space is extremely complex, meaning that a generated architecture can be of any length and scheme. More, in our experiments, we create a search space for each evaluated data set, as the CNNs yield different fitnesses for different problems. Also, by using information about the probabilities of state-transition and the inner-states, LCMNAS leverages existing information to efficiently guide the search and to design both the architecture and the layer's parameters without requiring heuristics. Future works can use this search space without leveraging such information and solely focus on the possible operations to design cell-based architectures.

4.4. Results and Discussion

To evaluate the proposed method, we conducted extensive experiments using a single 1080Ti GPU. First, following the best practices proposed, we evaluate the performance of Random Search (RS) to infer the complexity of the search space [29]. For this, we evaluate RS by randomly sampling architectures from the search space, \mathcal{A} , and two RSs based on the proposed evolutionary strategy: RS-L, that randomly samples layer components, and RS-M, that randomly samples models to serve as parents. The results

Architecture	CIFAR-10				CIFAR-100				ImageNet16-120				Search Method
	Test Error (%)	Inference Time (ms)	Search Cost (GPU days)	Params (M)	Test Error (%)	Inference Time (ms)	Search Cost (GPU days)	Params (M)	Test Error (%)	Inference Time (ms)	Search Cost (GPU days)	Params (M)	
ResNet	6.43	0.24 ± 0.19	-	1.7	29.14	0.21 ± 0.13	-	1.7	56.37	0.10 ± 0.19	-	1.7	Manual
NAS-Bench-201 Best Architecture	5.63	0.16 ± 0.13	-	1.1	26.49	0.18 ± 0.13	-	1.3	52.69	0.08 ± 0.12	-	0.9	-
RS-L	10.73	1.06 ± 0.10	0.27	34.4	31.95	0.28 ± 0.09	0.01	0.7	82.08	0.01 ± 0.01	0.26	0.5	RS
RS-M	21.67	0.09 ± 0.01	0.01	0.3	46.82	0.06 ± 0.01	0.01	0.8	60.02	0.03 ± 0.01	0.01	1.3	RS
RS	7.96	0.03 ± 0.01	0.01	0.6	47.33	0.01 ± 0.01	0.01	0.4	64.33	0.02 ± 0.01	0.01	0.7	RS
Ours ($\lambda=0$)	6.05	2.08 ± 0.04	1	43.9	29.44	1.67 ± 0.02	0.67	49.5	58.45	0.75 ± 0.01	1.29	224.7	EA
Ours ($\lambda=0.25$)	5.49	0.97 ± 0.02	1.23	32.5	28.27	0.92 ± 0.35	1.9	60.4	57.33	3.43 ± 0.04	3	171.1	EA
Ours ($\lambda=0.50$)	4.64	0.26 ± 0.04	1.36	13.9	25.45	1.81 ± 0.02	2.7	51.5	49.12	0.19 ± 0.01	5.01	12.8	EA
Ours ($\lambda=0.75$)	4.23	0.33 ± 0.01	1.03	6.7	25.99	0.39 ± 0.18	2.8	32.3	45.78	0.90 ± 0.01	4.79	42.7	EA
Ours ($\lambda=1$)	4.81	0.15 ± 0.01	0.1	2.5	26.52	0.16 ± 0.01	0.01	2.2	51.17	0.76 ± 0.01	0.12	31.5	EA
Ours (best) + AA †	2.96	0.33 ± 0.01	1.03	6.7	20.94	1.81 ± 0.02	2.7	51.5	43.35	0.90 ± 0.01	4.79	42.7	EA

† Results obtained by training the best model found in each data set: $\lambda = 0.75$ for CIFAR-10 and ImageNet16-120 and $\lambda = 0.5$ for CIFAR-100 with AutoAugment for 1500 epochs.

Table 1. Comparison of the proposed method against ResNet, the best architecture in NAS-Bench-201 benchmark and 3 types of random-search. The proposed method is evaluated using different λ values for the proposed mixed-performance estimation strategy. The comparison is measured, when applicable, by the test error (%), the inference time (ms), the search cost in GPU days and the number of parameters of the generated architecture (in millions).

for these three methods are shown in the second block of Table 1. As the three RSs attain high values for the test error, it shows that the search space is complex, and unlike other search spaces, RS is not sufficient to design competitive architectures [29, 67]. Then, we evaluated the proposed method, by giving different importance’s (λ) to the two components of the mixed-performance estimation. Results are presented in Table 1, third block. Following the best practices suggested in [67], we first present the test errors without any added training protocol. From these, we see that a combination of both evaluating an architecture based on its trainability using low-fidelity estimates, and its modelling capabilities at initialization stage, yields the best results. Moreover, higher λ values serve as regularization, reducing the number of parameters in the generated architectures. The search cost is lower when $\lambda = 1$, due to the fast evaluation of untrained networks. Differences in search cost between data sets are due to the unconstrained properties of the search. As for noisier data sets, larger models tend to be generated, thus taking more time to evaluate. Also, the larger size of ImageNet16-120 also slows the evaluation. For the best architecture found in each dataset ($\lambda = 0.75$ in CIFAR-10 and ImageNet16-120 and $\lambda = 0.5$ in CIFAR-100), we also show the test error by training the architecture for 1500 epochs with AutoAugment [9], attaining 2.96% test error in CIFAR-10, 20.94% in CIFAR-100 and 43.35% in ImageNet16-120. By comparing the proposed method with ResNet, and the best possible architecture in the NAS-Bench-201 (first block in Table 1), it is possible to see that the proposed method heavily outperforms existing state-of-the-art manually designed CNNs and all cell-based CNNs present in NAS-Bench-201. Moreover, comparing with RS is indicative of the effectiveness of the search, where the lower test error show that LCMNAS

effectively searches through the complex space of architectures.

Method	Test Error (%)	Search Cost (GPU Days)	Params (M)	Search Method
ResNet [16]	6.43	-	1.7	manual
ConvFabrics [52]	7.43	-	21.2	-
MetaQNN [2]	6.92	100	11.2	RL
NAS [74]	4.47	22400	7.1	RL
NAS + more filters [74]	3.65	22400	37.4	RL
Large-scale Evolution [49]	5.40	2750	5.4	EA
SMASH [3]	4.03	1.5	16.0	OS
Net Transformation [4]	5.70	10	19.7	RL
Super Nets [59]	9.21	-	-	-
ENAS [47]	4.23	0.32	21.3	RL
ENAS + more channels [47]	3.87	0.32	38.0	RL
EPNAS [46]	5.14	1.2	5.9	SMBO
NSGA-NET [43]	3.85	8	3.3	EA
RandGrow [18]	2.93	6	3.1	RS
LEMONADE [12]	3.60	80	8.9	EA
Petridish [19]	2.83	5	2.2	GB
Ours ($\lambda = 0.75$)+AA	2.96	1.03	6.7	EA

Table 2. Comparison of different methods on CIFAR-10. First block present a state-of-the-art human-designed CNN. Second block presents the results of proposals that perform macro-search. Third block presents the proposed method. For each method, the test error in percentages, the search cost in terms of GPU days and the size of the architecture in millions of parameters is shown. Cells with a slash mean that the categorization does not apply.

Table 2 compares the proposed method with different NAS methods that perform macro-search using CIFAR-10. It is important to note that most of these methods heavily rely on tuned search spaces and constraints, such as architecture skeletons, number of layers and forced initial and final operations, which has shown to hide the real contributions of the search strategy [67]. From this table, it is possible to see that LCMNAS achieves high performances (low

test error) while at the same time being orders of magnitude faster (search cost). LCMNAS closely relates with large-scale evolution [49], since both apply evolutionary strategies and heavily reduce the amount of human intervention in the decision process. By direct comparison, LCMNAS achieved a lower test error by 2.44%, while being orders of magnitude faster (2669x faster). By directly comparing with RandGrow and Petridish, the closest in terms of test error, we see that LCMNAS is 5x faster, while achieving similar test errors. However, RandGrow [18] and Petridish [19] rely on DropPath, which in RandGrow’s case, reduced its’ base test error from 3.38% to 2.93%. Regarding CIFAR-100, few proposals directly search on it, instead transfer architectures from CIFAR-10. As comparison, Large-scale evolution [49] achieved a test error of 23.7%, which is 2.76% higher than the 20.94% obtain by LCMNAS.

As most NAS methods focus on designing architectures in one data set and then transferring it to larger ones, we also study this using the best-generated architectures, without AutoAugment. However, contrary to common practices, we do not change the architectures when transferring them to emphasize the true contributions of the search strategy. What we found is that for similar data sets, i.e., CIFAR-10 and CIFAR-100, the architecture found in the first and transferred to the second, out-performs the architecture found directly searching on the second. We justify this due to the similar nature of the data sets, whereas CIFAR-100 is a more demanding data set, thus searching on that data set is harder. However, the same does not apply when transferring CIFAR-10 or CIFAR-100 to ImageNet16-120 and the other way around. The result of such transference falls heavily short when compared to directly searching in the desired data set. These results are shown in Table 3. From these, we conclude that directly searching is better than transferring if there are no similar and simpler data sets available that might aid in the search process.

Regarding the architecture’s design, a visualization of the best ones can be seen in the supplementary material. LCMNAS found that placing batch normalization layers after convolutional layers was an important building block, and usually ReLu also follows, meaning that after a convolutional layer, regularization layers are important. In CIFAR-10, LCMNAS specifically designed a very deep network with a small number of output channels, thus controlling the number of parameters. In the middle of this architecture, a dropout layer and a linear layer were added. We hypothesize that this served the purpose of regularization by not only dropping connections but also creating linear representations of the feature maps. In many architectures, a pattern of having convolutional layers with larger kernel sizes (7×7) interspersed with smaller ones (1×1 and 3×3) is seen. Also common to all architectures, LCMNAS tends to add dropout layers and reduction mechanisms, e.g., adap-

Searched On	Transferred To		
	CIFAR-10	CIFAR-100	ImageNet16-120
CIFAR-10	4.23	24.42	53.45
CIFAR-100	5.09	25.45	55.42
ImageNet16-120	8.15	30.39	45.78

Table 3. Test error (%) obtained by transferring the best architectures found in one data set to other data sets without any modifications. Architectures were trained on the new data set from scratch.

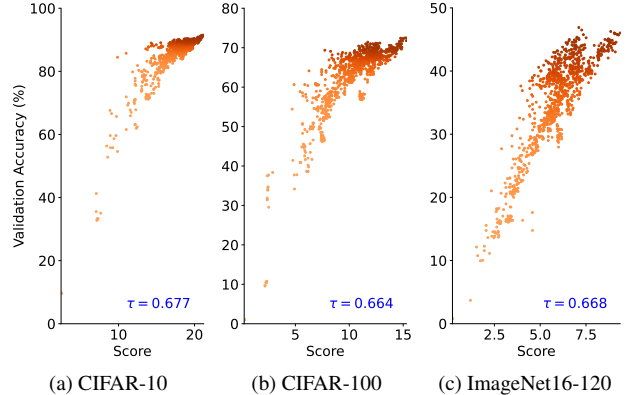


Figure 3. Kendall’s tau correlation (τ) between the proposed mixed-performance estimation and the final validation accuracy for the first 1000 architectures in all NAS-Bench-201 data sets.

tive average pooling, at the end of the architecture, especially in ImageNet16-120, a noisier data set.

4.5. Ablation Studies

We extend the studies on the proposed mixed-performance estimation strategy by looking at the Kendall’s tau correlation (τ) between the proposed mixed-performance estimation and the final validation accuracy for the first 1000 architectures in NAS-Bench-201 benchmark [11], results shown in Fig. 3. For all the data sets, the proposed method shows a high positive correlation, outperforming existing zero-proxy estimators [45].

We also evaluated the importance of the epochs used to partially train a generated architecture, using $\lambda = 0.75$ (results shown in Table 4). Naturally, reducing e implied an increase in the final test error and in the number of parameters of the final architecture. This can be justified by the difficulty in measuring the trainability of the architectures with low training epochs. Furthermore, in Table 5, we evaluated the impact of the number of generations, g , and population per generation, p , using $\lambda = 1$. The resulting test error shows that $g = 50$ and $p = 100$ yield the best results and that these parameters can influence the final result by a significant amount. In a perfect scenario, where computa-

tional costs are not considered, one could use a large e and evaluate more architectures by increasing g and p .

Finally, we ensemble the architectures found, using different λ values (Table 6) as indication of the architectures’ diversity [70]. Ensemble sizes k , go from the top-1 architecture ($k = 1$) to the top-5 architecture found. The resulting test error was obtained using weighted majority voting, with the accuracies attained while training used as weights. Results show that for all data sets evaluated, incrementally adding lower-performant architectures yields better results than the top-1 architecture alone. This experiment validates the premise that less constrained macro-search has benefits due to its’ inherent architecture generation diversity.

5. Conclusion

In this work, we propose a NAS approach that performs unconstrained macro-search. For this, we design three novel methods. For the search space design, we propose a method that autonomously generates complex search spaces by creating Weighted Directed Graphs with hidden properties from existing CNNs. The proposed search strategy performs macro-architecture search, via evolution, without requiring human-defined restrictions, such as outer-skeleton, initial architecture, or heuristics. To quickly evaluate generated architectures, we propose the use of a mixed-performance strategy that combines information about architectures at initialization stage with information about their validation accuracy after a partial train on a partial data set. Our experiments show that LCMNAS generates state-of-the-art architectures from scratch with minimal GPU computation, obtaining test errors of 2.96% in CIFAR-10, 20.94% in CIFAR-100 and 43.35% in ImageNet16-120. We also study the importance of different NAS components on a macro-search setting and draw insights from architecture design choices.

This work is not without limitations. We solely focused on the design of CNNs for image classification and did not study the use of multi-objective search as a regularization mechanism, as it was out of scope. However, we hope that this work serves the purpose of pushing NAS boundaries to less constrained spaces, where human-expertize for the design of inner-architecture parameters and search spaces is reduced, while at the same time generating architectures in a very efficient way, thus allowing a step towards widespread use of NAS for different problems and data sets.

Search Epochs e	CIFAR-10	
	Test Error (%)	Params (M)
$e = 1$	6.33	21.4
$e = 2$	4.92	170.1
$e = 3$	4.69	44.1
$e = 4$	4.23	6.7

Table 4. Test error (%) of the best architectures found on CIFAR-10, by using different search epochs e and $\lambda = 0.75$.

Parameters		CIFAR-10	
Generations (g)	Population (p)	Test Error (%)	Params (M)
5	5	16.52	0.3
10	10	5.46	3.9
10	25	5.25	3.6
10	50	6.97	0.9
10	100	6.83	12.7
15	15	6.08	0.4
15	25	5.58	8.7
15	50	6.16	7.6
15	100	5.37	13.9
25	25	5.49	2
25	50	6.52	3.1
25	100	4.97	8.4
50	50	5.24	4.7
50	100	4.81	2.5
100	50	6.69	5.3
100	100	5.94	13.6
100	250	5.54	55.9
150	150	6.19	3.3
150	250	6.46	2.2
250	100	5.27	36.1
250	250	6.14	4.8

Table 5. Test error (%) in CIFAR-10 using $\lambda = 1$ for different number of generations, g , and population sizes, p .

Ensemble Size (k)	Test Error (%)		
	CIFAR-10	CIFAR-100	ImageNet16-120
$k = 1$	4.23	25.45	45.78
$k = 2$	4.23	25.45	45.78
$k = 3$	3.67	22.64	44.67
$k = 4$	3.51	22.01	44.85
$k = 5$	3.59	21.52	44.72

Table 6. Ensemble test error (%) for CIFAR-10, CIFAR-100 and ImageNet-16-120 with different ensemble sizes k . Architectures used to perform the ensemble are the final ones found by searching with different $\lambda \in \{0, 0.25, 0.5, 0.75, 1\}$. $k = 1$ means using only the best architecture, while $k = 5$ uses all 5 architectures.

References

- [1] Torchvision. <https://pytorch.org/vision/0.8/models.html>, 2021. 5
- [2] Bowen Baker, Otkrist Gupta, Nikhil Naik, and Ramesh Raskar. Designing neural network architectures using reinforcement learning. In *ICLR*, 2017. 2, 3, 6
- [3] Andrew Brock, Theo Lim, J.M. Ritchie, and Nick Weston. SMASH: One-shot model architecture search through hyper-networks. In *ICLR*, 2018. 6
- [4] Han Cai, Tianyao Chen, Weinan Zhang, Yong Yu, and Jun Wang. Efficient architecture search by network transformation. In *AAAI*, 2018. 3, 6
- [5] Han Cai, Ligeng Zhu, and Song Han. Proxylessnas: Direct neural architecture search on target task and hardware. In *ICLR*, 2019. 1, 2, 3
- [6] Wuyang Chen, Xinyu Gong, and Zhangyang Wang. Neural architecture search on imagenet in four gpu hours: A theoretically inspired perspective. In *ICLR*, 2021. 3
- [7] Xin Chen, Lingxi Xie, Jun Wu, and Qi Tian. Progressive differentiable architecture search: Bridging the depth gap between search and evaluation. In *ICCV*, 2019. 2
- [8] Yukang Chen, Tong Yang, Xiangyu Zhang, Gaofeng Meng, Xinyu Xiao, and Jian Sun. Detnas: Backbone search for object detection, 2019. 1
- [9] Ekin D Cubuk, Barret Zoph, Dandelion Mane, Vijay Vasudevan, and Quoc V Le. Autoaugment: Learning augmentation policies from data. In *CVPR*, 2019. 6
- [10] Terrance DeVries and Graham W Taylor. Improved regularization of convolutional neural networks with cutout. *arXiv preprint arXiv:1708.04552*, 2017. 5
- [11] Xuanyi Dong and Yi Yang. NAS-Bench-201: Extending the Scope of Reproducible Neural Architecture Search. In *ICLR*, 2020. 2, 5, 7
- [12] Thomas Elsken, Jan Hendrik Metzen, and Frank Hutter. Efficient multi-objective neural architecture search via lamarckian evolution. In *ICLR*, 2019. 3, 6
- [13] Thomas Elsken, Jan Hendrik Metzen, and Frank Hutter. Neural architecture search: A survey. *Journal of Machine Learning Research*, 2019. 1, 2
- [14] Chen Gao, Yunpeng Chen, Si Liu, Zhenxiong Tan, and Shuicheng Yan. Adversarialnas: Adversarial neural architecture search for gans. In *CVPR*, 2020. 1
- [15] Xinyu Gong, Shiyu Chang, Yifan Jiang, and Zhangyang Wang. Autogan: Neural architecture search for generative adversarial networks. In *ICCV*, 2019. 1
- [16] Kaiming He, Xiangyu Zhang, Shaoqing Ren, and Jian Sun. Deep residual learning for image recognition. In *CVPR*, 2016. 6, 11
- [17] Andrew Howard, Mark Sandler, Grace Chu, Liang-Chieh Chen, Bo Chen, Mingxing Tan, Weijun Wang, Yukun Zhu, Ruoming Pang, Vijay Vasudevan, et al. Searching for mobilenetv3. In *ICCV*, 2019. 2
- [18] Hanzhang Hu, John Langford, Rich Caruana, Eric Horvitz, and Debadeepta Dey. Macro neural architecture search revisited. In *NeurIPS Workshop on Meta-Learning*, 2018. 3, 6, 7
- [19] Hanzhang Hu, John Langford, Rich Caruana, Saurajit Mukherjee, Eric J Horvitz, and Debadeepta Dey. Efficient forward architecture search. In *NeurIPS*, 2019. 3, 6, 7
- [20] Gao Huang, Zhuang Liu, Laurens Van Der Maaten, and Kilian Q Weinberger. Densely connected convolutional networks. In *CVPR*, 2017. 11
- [21] Frank Hutter, Lars Kotthoff, and Joaquin Vanschoren. *Automated Machine Learning*. Springer, 2019. 1
- [22] Forrest N Iandola, Song Han, Matthew W Moskewicz, Khalid Ashraf, William J Dally, and Kurt Keutzer. Squeezenet: Alexnet-level accuracy with 50x fewer parameters and 0.5 mb model size. *arXiv preprint arXiv:1602.07360*, 2016. 11
- [23] Kirthevasan Kandasamy, Willie Neiswanger, Jeff Schneider, Barnabás Póczos, and Eric P. Xing. Neural architecture search with bayesian optimisation and optimal transport. In *NeurIPS*, 2018. 3
- [24] Asifullah Khan, Anabia Sohail, Umme Zahoora, and Aqsa Saeed Qureshi. A survey of the recent architectures of deep convolutional neural networks. *Artificial Intelligence Review*, 53(8):5455–5516, 2020. 1
- [25] Alex Krizhevsky, Geoffrey Hinton, et al. Learning multiple layers of features from tiny images. Technical report, Cite-seer, 2009. 5
- [26] Alex Krizhevsky, Ilya Sutskever, and Geoffrey E Hinton. Imagenet classification with deep convolutional neural networks. In *NeurIPS*, 2012. 11
- [27] Gustav Larsson, Michael Maire, and Gregory Shakhnarovich. Fractalnet: Ultra-deep neural networks without residuals. In *ICLR*, 2017. 5
- [28] Yann LeCun, Yoshua Bengio, and Geoffrey Hinton. Deep learning. *Nature*, 2015. 1
- [29] Liam Li and Ameet Talwalkar. Random search and reproducibility for neural architecture search. In *UAI*, 2019. 2, 3, 5, 6
- [30] Zhihang Li, Teng Xi, Jiankang Deng, Gang Zhang, Shengzhao Wen, and Ran He. Gp-nas: Gaussian process based neural architecture search. In *CVPR*, June 2020. 3
- [31] Marius Lindauer and Frank Hutter. Best practices for scientific research on neural architecture search. *CoRR*, abs/1909.02453, 2019. 5
- [32] Chenxi Liu, Liang-Chieh Chen, Florian Schroff, Hartwig Adam, Wei Hua, Alan L Yuille, and Li Fei-Fei. Auto-deeplab: Hierarchical neural architecture search for semantic image segmentation. In *CVPR*, 2019. 1
- [33] Chenxi Liu, Piotr Dollár, Kaiming He, Ross B. Girshick, Alan L. Yuille, and Saining Xie. Are labels necessary for neural architecture search? In *ECCV*, 2020. 1
- [34] Chenxi Liu, Barret Zoph, Maxim Neumann, Jonathon Shlens, Wei Hua, Li-Jia Li, Li Fei-Fei, Alan L. Yuille, Jonathan Huang, and Kevin Murphy. Progressive neural architecture search. In *ECCV*. 3
- [35] Hanxiao Liu, Karen Simonyan, Oriol Vinyals, Chrisantha Fernando, and Koray Kavukcuoglu. Hierarchical Representations for Efficient Architecture Search. In *ICLR*, 2018. 2
- [36] Hanxiao Liu, Karen Simonyan, and Yiming Yang. DARTS: Differentiable architecture search. In *ICLR*, 2019. 1, 2, 5

- [37] Yuqiao Liu, Yanan Sun, Bing Xue, Mengjie Zhang, Gary G Yen, and Kay Chen Tan. A survey on evolutionary neural architecture search. *IEEE TNNLS*, 2021. 1, 2
- [38] Vasco Lopes and Luís A Alexandre. Auto-classifier: A robust defect detector based on an automl head. In *International Conference on Neural Information Processing*, pages 137–149. Springer, Cham, 2020. 1
- [39] Vasco Lopes, Saeid Alirezazadeh, and Luís A. Alexandre. EPE-NAS: efficient performance estimation without training for neural architecture search. In *ICANN*, 2021. 3, 4
- [40] Vasco Lopes, António Gaspar, Luís A Alexandre, and João Cordeiro. An automl-based approach to multimodal image sentiment analysis. In *International Joint Conference on Neural Networks (IJCNN)*, 2021. 1
- [41] Vasco Lopes, Miguel Santos, Bruno Degardin, and Luís A Alexandre. Guided evolution for neural architecture search. In *Advances in Neural Information Processing Systems 35 (NeurIPS) - New In ML*, 2021. 2
- [42] Ilya Loshchilov and Frank Hutter. SGDR: stochastic gradient descent with warm restarts. In *ICLR*, 2017. 5
- [43] Zhichao Lu, Ian Whalen, Vishnu Boddeti, Yashesh D. Dhebar, Kalyanmoy Deb, Erik D. Goodman, and Wolfgang Banzhaf. Nsga-net: Neural architecture search using multi-objective genetic algorithm. In Anne Auger and Thomas Stützle, editors, *GECCO*, 2019. 3, 6
- [44] Ningning Ma, Xiangyu Zhang, Hai-Tao Zheng, and Jian Sun. Shufflenet v2: Practical guidelines for efficient cnn architecture design. In *ECCV*, 2018. 11
- [45] Joe Mellor, Jack Turner, Amos J. Storkey, and Elliot J. Crowley. Neural architecture search without training. In Marina Meila and Tong Zhang, editors, *ICML*, 2021. 3, 4, 7
- [46] Juan-Manuel Perez-Rua, Moez Baccouche, and Stéphane Pateux. Efficient progressive neural architecture search. In *British Machine Vision Conference*, 2018. 6
- [47] Hieu Pham, Melody Guan, Barret Zoph, Quoc Le, and Jeff Dean. Efficient neural architecture search via parameters sharing. In *ICML*, 2018. 2, 3, 5, 6
- [48] Esteban Real, Alok Aggarwal, Yanping Huang, and Quoc V Le. Regularized Evolution for Image Classifier Architecture Search. In *AAAI*, 2019. 2, 4, 5
- [49] Esteban Real, Sherry Moore, Andrew Selle, Saurabh Saxena, Yutaka Leon Suematsu, Jie Tan, Quoc V Le, and Alexey Kurakin. Large-scale evolution of image classifiers. In *ICML*, 2017. 3, 6, 7
- [50] Pengzhen Ren, Yun Xiao, Xiaojun Chang, Poyao Huang, Zhihui Li, Xiaojiang Chen, and Xin Wang. A comprehensive survey of neural architecture search: Challenges and solutions. *ACM Comput. Surv.*, 2021. 1
- [51] Mark Sandler, Andrew Howard, Menglong Zhu, Andrey Zhmoginov, and Liang-Chieh Chen. Mobilenetv2: Inverted residuals and linear bottlenecks. In *CVPR*, 2018. 11
- [52] Shreyas Saxena and Jakob Verbeek. Convolutional neural fabrics. In *NeurIPS*, 2016. 6
- [53] Jürgen Schmidhuber. Deep Learning in Neural Networks: An Overview. *Neural networks*, 2015. 1
- [54] Julien Siems, Lucas Zimmer, Arber Zela, Jovita Lukasik, Margret Keuper, and Frank Hutter. Nas-bench-301 and the case for surrogate benchmarks for neural architecture search. *arXiv:2008.09777*, 2020. 2
- [55] Karen Simonyan and Andrew Zisserman. Very deep convolutional networks for large-scale image recognition. In *ICLR*, 2015. 11
- [56] Ilya Sutskever, James Martens, George E. Dahl, and Geoffrey E. Hinton. On the importance of initialization and momentum in deep learning. In *ICML*, 2013. 5
- [57] Christian Szegedy, Wei Liu, Yangqing Jia, Pierre Sermanet, Scott Reed, Dragomir Anguelov, Dumitru Erhan, Vincent Vanhoucke, and Andrew Rabinovich. Going deeper with convolutions. In *CVPR*, 2015. 11
- [58] Mingxing Tan, Bo Chen, Ruoming Pang, Vijay Vasudevan, Mark Sandler, Andrew Howard, and Quoc V Le. Mnasnet: Platform-aware neural architecture search for mobile. In *CVPR*, 2019. 11
- [59] Tom Veniat and Ludovic Denoyer. Learning time/memory-efficient deep architectures with budgeted super networks. In *CVPR*, 2018. 6
- [60] Xingchen Wan, Binxin Ru, Pedro M Esperança, and Zhen-guo Li. On redundancy and diversity in cell-based neural architecture search. In *ICLR*, 2022. 2, 3, 5
- [61] Colin White, Willie Neiswanger, and Yash Savani. BANANAS: bayesian optimization with neural architectures for neural architecture search. In *AAAI*, 2021. 3
- [62] Colin White, Arber Zela, Binxin Ru, Yang Liu, and Frank Hutter. How powerful are performance predictors in neural architecture search? In *NeurIPS*, 2021. 3
- [63] Saining Xie, Ross Girshick, Piotr Dollár, Zhuowen Tu, and Kaiming He. Aggregated residual transformations for deep neural networks. In *CVPR*, 2017. 11
- [64] Sirui Xie, Hehui Zheng, Chunxiao Liu, and Liang Lin. SNAS: stochastic neural architecture search. In *ICLR*, 2019. 2, 3
- [65] Xiangning Xie, Yuqiao Liu, Yanan Sun, Gary G Yen, Bing Xue, and Mengjie Zhang. Benchenas: A benchmarking platform for evolutionary neural architecture search. *arXiv:2108.03856*, 2021. 2
- [66] Yuhui Xu, Lingxi Xie, Xiaopeng Zhang, Xin Chen, Guo-Jun Qi, Qi Tian, and Hongkai Xiong. Pc-darts: Partial channel connections for memory-efficient architecture search. In *ICLR*, 2020. 2
- [67] Antoine Yang, Pedro M. Esperança, and Fabio M. Carlucci. Nas evaluation is frustratingly hard. In *ICLR*, 2020. 2, 3, 5, 6
- [68] Chris Ying, Aaron Klein, Eric Christiansen, Esteban Real, Kevin Murphy, and Frank Hutter. NAS-bench-101: Towards reproducible neural architecture search. In *ICML*. 2
- [69] Sergey Zagoruyko and Nikos Komodakis. Wide residual networks. *British Machine Vision Conference*, 2016. 11
- [70] Sheheryar Zaidi, Arber Zela, Thomas Elsken, Chris Holmes, Frank Hutter, and Yee Whye Teh. Neural Ensemble Search for Performant and Calibrated Predictions. *arXiv:2006.08573*, 2020. 8
- [71] Arber Zela, Thomas Elsken, Tonmoy Saikia, Yassine Marakchi, Thomas Brox, and Frank Hutter. Understanding and Robustifying Differentiable Architecture Search. In *ICLR*, 2020. 1, 2

- [72] Arber Zela, Aaron Klein, Stefan Falkner, and Frank Hutter. Towards automated deep learning: Efficient joint neural architecture and hyperparameter search. In *ICML Workshop on AutoML*, 2018. 3
- [73] Zhao Zhong, Junjie Yan, Wei Wu, Jing Shao, and Cheng-Lin Liu. Practical Block-Wise Neural Network Architecture Generation. In *CVPR*, 2018. 2
- [74] Barret Zoph and Quoc V. Le. Neural architecture search with reinforcement learning. In *ICLR*, 2017. 2, 3, 4, 6
- [75] Barret Zoph, Vijay Vasudevan, Jonathon Shlens, and Quoc V. Le. Learning transferable architectures for scalable image recognition. In *CVPR*, 2018. 2, 3, 4

A. Visualization of the Best Architectures Found

Figs. 4, 5, 6, show the architecture of the best models found by searching on CIFAR-10, CIFAR-100 and

ImageNet16-120, respectively.

B. Search Space - Models

In detail, the models used were: AlexNet [26], DenseNet{121,161,169,201} [20], GoogLeNet [57], MNASNet{0.5,0.75,1,1.3} [58], MobileNetv2 [51], ResNet{18,34,50,101,152} [16], ResNext{50,101} [63], ShuffleNetv2{0.5,1.0,1.5,2.0} [44], SqueezeNet{1.0,2.0} [22], VGG{11,11BN,13,13BN,16,16BN,19,19BN} [55] and Wide ResNet{50, 101} [69].

In Fig. 7, the Weighted Directed Graph with hidden properties (WDG) of DenseNet121 is presented, where layers are the nodes and connecting edges represent state-transition probabilities.

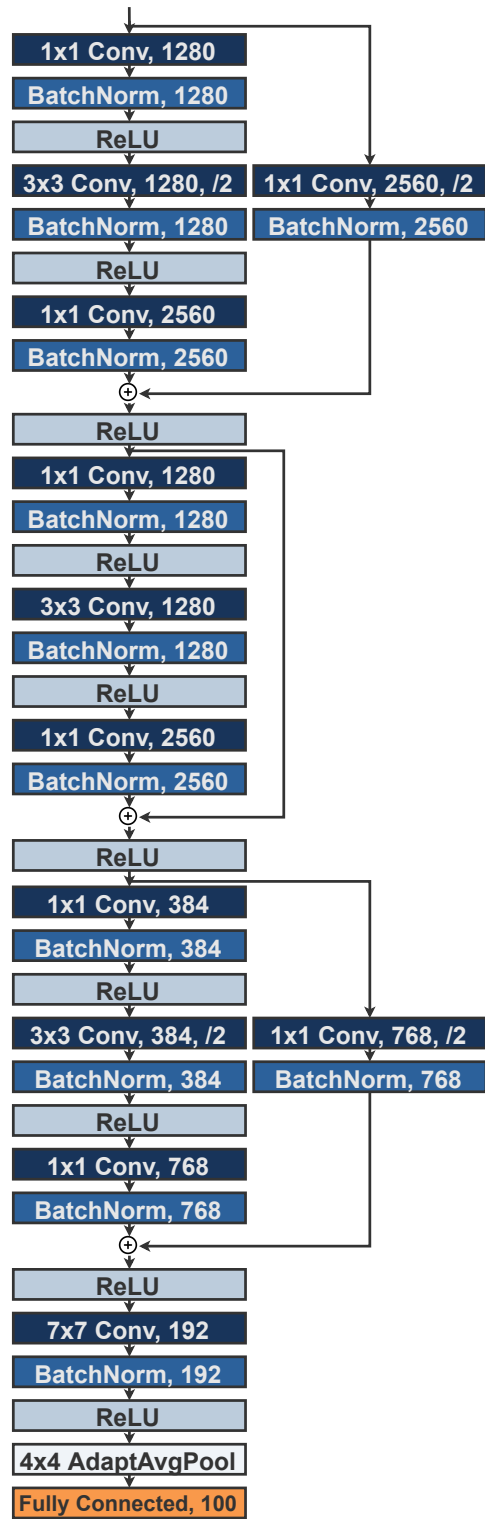
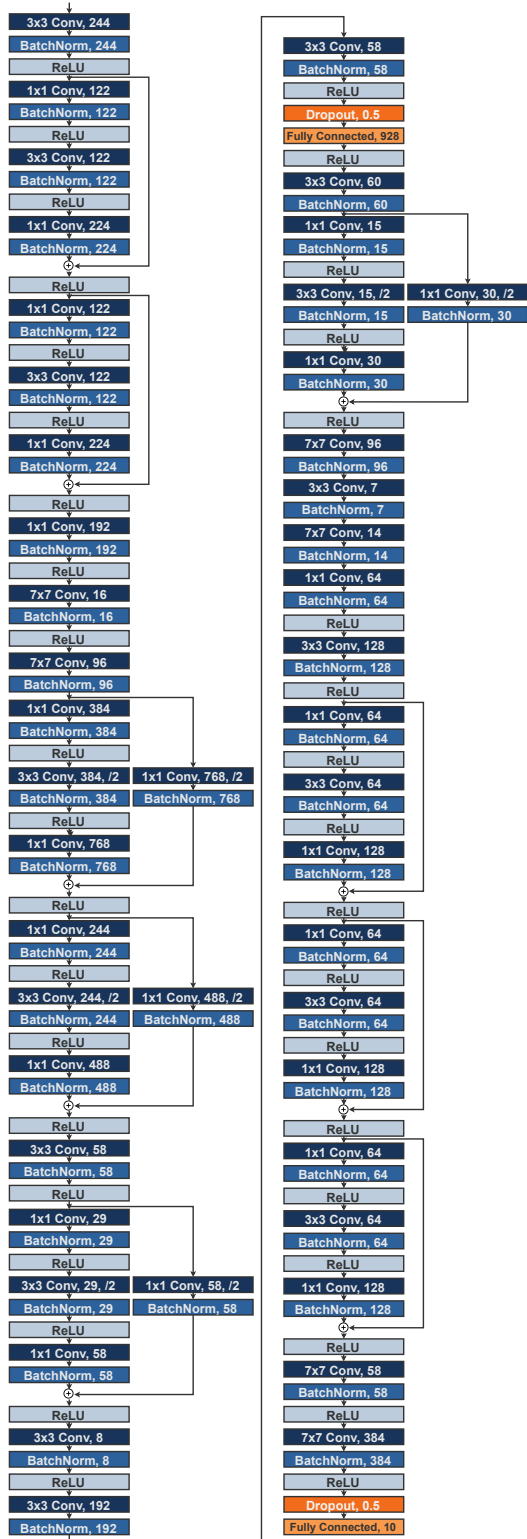


Figure 4. Architecture of the best model found in CIFAR-10 ($\lambda = 0.75$).

Figure 5. Architecture of the best model found in CIFAR-100 ($\lambda = 0.50$).

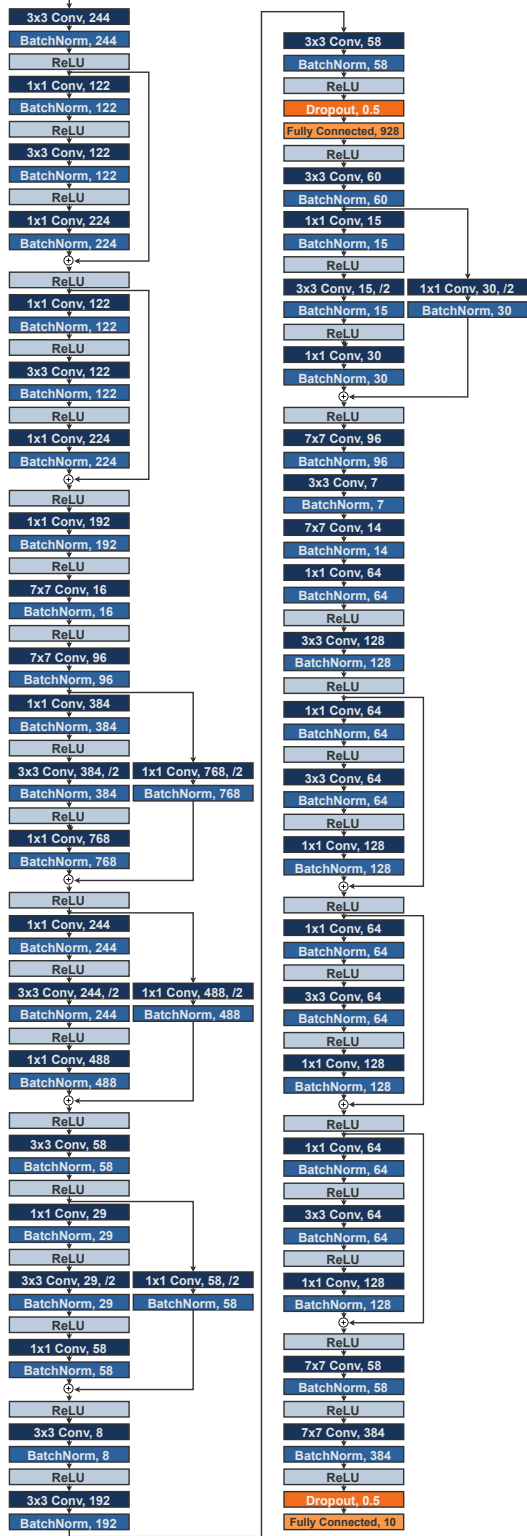


Figure 6. Architecture of the best model found in ImageNet16-120 ($\lambda = 0.75$).

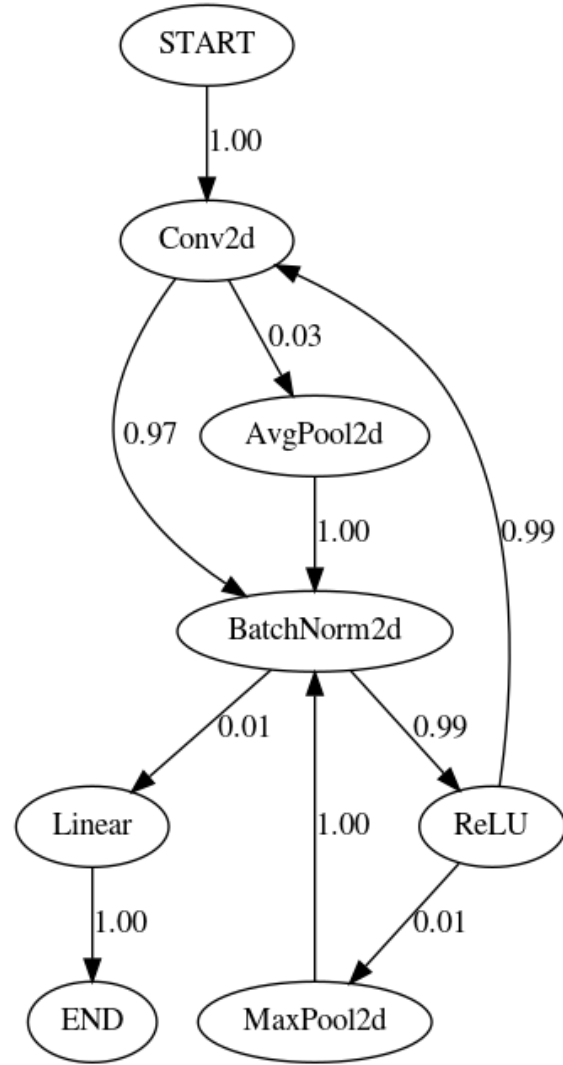


Figure 7. Weighted Directed Graph representation of DenseNet121. Nodes represent layers and edges represent state-transition probabilities.